

# Speed Estimation Techniques in Cellular Systems: Unified Performance Analysis

Ali Abdi<sup>1</sup>, Hong Zhang<sup>1</sup>, and Cihan Tepedelenlioglu<sup>2</sup>

<sup>1</sup>Dept. of Elec. and Comp. Eng., New Jersey Institute of Technology, Newark, NJ 07102, USA

<sup>2</sup>Dept. of Elec. Eng., Arizona State University, Tempe, AZ 85287, USA

Emails: ali.abdi@njit.edu, hz7@njit.edu, cihan@asu.edu

**Abstract** – Estimation of the mobile speed, or equivalently, the maximum Doppler frequency, is of importance in a variety of applications in wireless mobile communications. In this paper, a unified framework for the performance analysis of several major speed estimation techniques is presented, which allows a fair comparison between all the methods, analytically. Interestingly, it is proved that all these methods are equivalent, asymptotically, i.e., for large observation intervals. In addition, we have derived closed-form expressions for the bias and variance of a recently proposed covariance-based method. We have also introduced a new estimator which relies on the average number of maxima of the inphase component, and have calculated its variance, analytically. Our extensive performance analysis, supported by Monte Carlo simulations, have revealed that depending on the channel conditions, one needs to use a crossing- or a covariance-based technique, to achieve the desired estimation accuracy over a large range of mobile speeds.

## I. INTRODUCTION

Having an accurate estimate of the mobile speed, which provides information about the rate of change of the channel, is essential for handoff, dynamic channel assignment, adaptive transmission, power control, geolocation applications, etc.

There are two major classes of speed estimation techniques: crossing-based methods and covariance-based methods [1]. Some of these techniques have been extensively used so far. However, analytic performance analysis of some of these techniques, which helps the system designer to choose among different methods without extensive Monte Carlo simulations, is missing. In this paper we consider four crossing-based and two covariance-based schemes, and present a unified theoretical performance analysis framework.

The rest of this paper is organized as follows. The channel model is discussed in Section II. In Section III all the six estimators are derived and their bias properties are discussed. Section IV presents the unified performance analysis framework, along with exact variance expressions for the inphase-based methods and some asymptotic results. Simulations of the envelope-based techniques, for which theoretical performance analysis is not tractable, are given in Section V, along with a comprehensive performance comparison of all the methods. Section VI concludes the paper.

## II. THE CHANNEL MODEL

In a noisy Rician frequency-flat fading channel, with two-dimensional propagation of planar waves, the lowpass complex envelope at the mobile station (MS), downlink, can be written as

$$z(t) = x(t) + n(t), \quad (1)$$

where the complex process  $n(t)$  represents the noise, whereas the complex process  $x(t)$  includes the random diffuse component  $h(t)$  and the deterministic line-of-sight (LOS) component [1]

$$x(t) = \sqrt{\frac{\Omega}{K+1}} h(t) + \sqrt{\frac{K\Omega}{K+1}} \exp[j\omega_D \cos(\phi_0)t + \psi_0]. \quad (2)$$

In the above equation,  $h(t)$  is the superposition of a large number of multipath components, satisfying the central limit theorem, such that  $h(t)$  is a zero-mean unit-power complex Gaussian process, i.e.,  $E[|h(t)|^2] = 1$ . Moreover,  $\omega_D = 2\pi f_D = 2\pi v/\lambda = 2\pi v f_c/c$  is the maximum Doppler frequency in rad/sec,  $v$  is the MS speed,  $\lambda$  is the wavelength,  $f_c$  is the carrier frequency, and  $c$  is the speed of light. We also have  $j^2 = -1$ , and  $\phi_0$  and  $\psi_0$  stand for the angle-of-arrival (AOA) in the two-dimensional plane and the phase of the LOS component, respectively. In eq. (2),  $\Omega = E[|x(t)|^2]$  is the total received power, whereas the Rice factor  $K$  is the ratio of the LOS power to the diffuse power of  $x(t)$ . For the received signal at the base station (BS), uplink, the same equations as (1) and (2) hold [2].

For complete characterization of  $h(t)$ , we need the corresponding correlation function,  $r_h(\tau) = E[h(t)h^*(t+\tau)]$ , which is given by

$$r_h(\tau) = \int_{-\pi}^{\pi} p_h(\phi) \exp[-j\omega_D \cos(\phi)\tau] d\phi, \quad (3)$$

where  $p_h(\phi)$  is the probability density function (PDF) of the AOA in the two-dimensional plane. For  $r_x(\tau) = E[x(t)x^*(t+\tau)]$  we have

$$r_x(\tau) = \frac{\Omega}{K+1} r_h(\tau) + \frac{K\Omega}{K+1} \exp[-j\omega_D \cos(\phi_0)\tau]. \quad (4)$$

For isotropic scattering, i.e.,  $p_h(\phi) = 1/(2\pi)$ , we obtain Clarke's correlation model  $r_h(\tau) = J_0(\omega_D \tau)$ , with  $J_0(\cdot)$  as the zero-order Bessel function of the first kind. However, in the presence of nonisotropic scattering,  $p_h(\phi)$  and consequently  $r_h(\tau)$  could be very far from the uniform PDF and Clarke's model, respectively. The von Mises PDF has proven to be a flexible model for the nonuniform distribution of AOA both at the MS and the BS, studied in [3] and [2], respectively

$$p_h(\phi) = \exp[\kappa \cos(\phi - \alpha)] / [2\pi I_0(\kappa)], \quad \phi \in [-\pi, \pi], \quad (5)$$

where  $\alpha \in [-\pi, \pi]$  accounts for the mean direction of AOA of multipath components,  $\kappa \geq 0$  controls the width of the AOA of multipath components, and  $I_0(\cdot)$  is the zero-order modified Bessel function of the first kind. For this AOA distribution, the correlation function at the MS can be shown to be [3]

$$r_h(\tau) = I_0\left(\sqrt{\kappa^2 - \omega_D^2 \tau^2 + j2\kappa \cos(\alpha)\omega_D \tau}\right) / I_0(\kappa). \quad (6)$$

The same result holds for the BS [2].

In general, the noise process  $n(t)$  in (1) is composed of two parts: the receiver noise and the man-made noise [4]. The receiver noise is commonly modeled as a Gaussian process, whereas the man-made noise, generated by electrical equipments such as the vehicle ignition system, neon signs, etc., has an impulsive non-Gaussian characteristic, very different from the Gaussian noise, and appears in the frequency spectrum up to 7 GHz [4]. Apparently the man-made noise has received no attention in the context of speed estimation, and

is a topic of our current research. It seems that crossing-based methods are less sensitive to the impulsive noise.

### III. SPEED ESTIMATION: A CONTINUOUS-TIME APPROACH

In this section we adopt the basic propagation mechanism of isotropic scattering with no LOS in a noise-free environment, which entails straightforward derivation and performance analysis of a variety of existing and new speed estimation techniques under the same umbrella. The effect of nonisotropic scattering and Gaussian noise will be studied later, either via analytic methods or simulation.

In the absence of noise and LOS,  $K=0$ , and assuming  $\Omega=1$ , unit received power, one gets  $z(t)=x(t)=h(t)$  for the received signal according to (1) and (2). So, in this section we just concentrate on  $h(t)$ . In what follows and with  $r_h(\tau)=J_0(\omega_D\tau)$ , we consider two classes of estimation methods: crossing-based and covariance-based techniques. Since the vehicle speed  $v$  is proportional to the maximum Doppler frequency  $\omega_D$ , in the rest of the paper we attempt on estimating  $\omega_D$ , to simplify the notation. We may use either  $\xi(t)=\Re\{h(t)\}$ , the inphase component, where  $\Re\{\cdot\}$  gives the real part, or  $\eta(t)=|h(t)|^2$ , the envelope-squared, each one observed over a time interval of length  $T$ . Note that  $\xi(t)$  is a zero-mean real Gaussian process with variance  $1/2$ , whereas  $\eta(t)$  has an exponential distribution, i.e.,  $p(\eta)=\exp(-\eta)$ . We use  $|h(t)|^2$  rather than  $|h(t)|$ , the envelope, as the correlation function of envelope-squared in some cases of interest can be expressed in simple closed forms [5], required for analytic studies. For  $r_\xi(\tau)=E[\xi(t)\xi(t+\tau)]$  we have  $r_\xi(\tau)=(1/2)\Re\{r_h(\tau)\}$ . On the other hand, for  $r_\eta(\tau)=E[\eta(t)\eta(t+\tau)]$ , it is shown that  $r_\eta(\tau)=1+|r_h(\tau)|^2$  [5]. Hence, with  $r_h(\tau)=J_0(\omega_D\tau)$ , we obtain  $r_\xi(\tau)=(1/2)J_0(\omega_D\tau)$  and  $r_\eta(\tau)=1+J_0^2(\omega_D\tau)$ .

Last but not the least, note that rather than working with the sampled version of  $h(t)$ , i.e.,  $h[\ell]=h(\ell T_s)$ ,  $\ell=0,1,2,\dots$ , with  $T_s$  as the sampling period, we work with the continuous-time process itself, which allows us to derive closed-form results for the variance of the estimators. The effect of sampling, briefly discussed in [6], is negligible as long as  $T_s$  is small enough.

#### A. Crossing-Based Methods

For a given real random process  $y(t)$ , let us define  $N_y(y_h, T)$  as the number of times that the process crosses the threshold level  $y_h$ , with positive slope, over the time interval  $(0, T]$ . Also let  $M_y(T)$  denote the number of maxima of the process  $y(t)$  over the time interval  $(0, T]$ . For the zero crossing and the maxima of  $\xi(t)$ , the following results can be derived from [5] and [7], respectively

$$E[N_\xi(0, T)] = T\omega_D / (2\pi\sqrt{2}), \quad (7)$$

$$E[M_\xi(T)] = T\omega_D\sqrt{3}/(4\pi). \quad (8)$$

On the other hand, for the level crossing and the maxima of  $\eta(t)$ , one can obtain the following results from [5] and [8], respectively

$$E[N_\eta(1, T)] = T\omega_D / (e\sqrt{2\pi}), \quad (9)$$

$$E[M_\eta(T)] = T\omega_D 3/(4\pi). \quad (10)$$

Based on (7)-(10), the following estimators can be considered

$$\hat{\omega}_{D,1} = (2\pi\sqrt{2}) N_\xi(0, T) T^{-1}, \quad (11)$$

$$\hat{\omega}_{D,2} = (4\pi/\sqrt{3}) M_\xi(T) T^{-1}, \quad (12)$$

$$\hat{\omega}_{D,3} = (e\sqrt{2\pi}) N_\eta(1, T) T^{-1}, \quad (13)$$

$$\hat{\omega}_{D,4} = (4\pi/3) M_\eta(T) T^{-1}. \quad (14)$$

All these four estimators are unbiased, i.e.,  $E[\hat{\omega}_{D,i}] = \omega_D$ ,  $i=1,\dots,4$ . According to the literature survey of [1] and among these four crossing-based estimators,  $\hat{\omega}_{D,2}$  which employs the number of maxima of the inphase component appears to be new.

#### B. Covariance-Based Methods

##### B.1. Covariance matching method

Based on the covariance function definitions  $c_\xi(\tau)=r_\xi(\tau)-\{E[\xi(t)]\}^2$  and  $c_\eta(\tau)=r_\eta(\tau)-\{E[\eta(t)]\}^2$ , along with  $r_\xi(\tau)=(1/2)J_0(\omega_D\tau)$ ,  $r_\eta(\tau)=1+J_0^2(\omega_D\tau)$ ,  $E[\xi(t)]=0$ , and  $E[\eta(t)]=1$ , one obtains

$$c_\xi(\tau) = (1/2)J_0(\omega_D\tau), \quad (15)$$

$$c_\eta(\tau) = J_0^2(\omega_D\tau). \quad (16)$$

According to Taylor expansion we have  $J_0(\omega_D\tau) = 1 - (\omega_D^2/4)\tau^2 + O(\tau^4)$ , as  $\tau \rightarrow 0$ , where  $f_1(t) = O(f_2(t))$  as  $t \rightarrow 0$  means that  $f_1(t)/f_2(t)$  is bounded in a neighborhood around zero. Therefore

$$c_\xi(\tau) = (1/2) - (\omega_D^2/8)\tau^2 + O(\tau^4), \text{ as } \tau \rightarrow 0, \quad (17)$$

$$c_\eta(\tau) = 1 - (\omega_D^2/2)\tau^2 + O(\tau^4), \text{ as } \tau \rightarrow 0. \quad (18)$$

The quadratic form of the covariance functions in (17) and (18) for small  $\tau$ , i.e.,  $c_y(\tau) \approx a - b\omega_D^2\tau^2$ , where  $a=1/2, 1$  and  $b=1/8, 1/2$  for  $y(t)=\xi(t), \eta(t)$ , respectively, motivates to estimate  $\omega_D^2$  by fitting a quadratic equation  $a - b\omega_D^2\tau^2$  to the sample covariance function,  $\hat{c}_y(\tau)$ , via a minimum mean squared error (MMSE) procedure, i.e.

$$\min_{\omega_D^2} E \left\{ \int_0^{T_0} [\hat{c}_y(\tau) - a + b\omega_D^2\tau^2]^2 d\tau \right\}, \quad (19)$$

where  $T_0$  is sufficiently small. By setting the derivative (with respect to  $\omega_D^2$ ) of the expectation in (19) to zero, the MMSE estimate of  $\omega_D^2$  can be shown to be

$$\hat{\omega}_{D,5}^2 = \frac{5a}{3bT_0^2} - \frac{5}{bT_0^5} \int_0^{T_0} \tau^2 \hat{c}_y(\tau) d\tau. \quad (20)$$

The natural choice for estimating  $\omega_D$  from (20) is

$$\hat{\omega}_{D,5} = \sqrt{\hat{\omega}_{D,5}^2}. \quad (21)$$

Obviously this is a biased estimator for  $\omega_D$ . To be able to calculate the bias approximately, using the same argument as [6], assume the variance of the estimator is small enough, which allows a first-order Taylor expansion for  $\sqrt{\hat{\omega}_{D,5}^2}$  around  $E[\hat{\omega}_{D,5}^2]$ , which implies that  $E[\hat{\omega}_{D,5}] \approx \sqrt{E[\hat{\omega}_{D,5}^2]}$ . With this unbiased estimator

$$\hat{c}_y(\tau) = \frac{1}{T} \int_0^T y(t)y(t+\tau)dt, \quad (22)$$

we get

$$E[\hat{\omega}_{D,5}^2] = \frac{5a}{3bT_0^2} - \frac{5}{bT_0^5} \int_0^{T_0} \tau^2 c_y(\tau) d\tau. \quad (23)$$

Based on  $c_y(\tau) = a - b\omega_D^2\tau^2 + O(\tau^4)$ , as  $\tau \rightarrow 0$ , with  $a$  and  $b$  defined after (17) and (18), eq. (23) can be written as

$$E[\hat{\omega}_{D,5}^2] = \omega_D^2 + O(T_0^2), \text{ as } T_0 \rightarrow 0. \quad (24)$$

Since  $\sqrt{1+t} = 1 + O(t)$ , as  $t \rightarrow 0$ , we eventually come up the following result for the bias of  $\hat{\omega}_{D,5}$ , valid for both  $\xi(t)$  and  $\eta(t)$

$$E[\hat{\omega}_{D,5}] \approx \omega_D + O(T_0^2), \text{ as } T_0 \rightarrow 0. \quad (25)$$

Clearly this approximate-asymptotic result, derived analytically, is supposed to provide just an insight into the bias behavior of  $\hat{\omega}_{D,5}$  with respect to  $T_0$ . The approximation  $E[\hat{\omega}_{D,5}] \approx \sqrt{E[\hat{\omega}_{D,5}^2]}$ , with  $E[\hat{\omega}_{D,5}^2]$  given by (23), is useful for any  $T_0$ . More conclusions can be

made only via Monte Carlo simulation. Also note that for a good-quality estimate of  $c_y(\tau)$ ,  $T$  in (22) should be much larger than  $T_0$ .

The idea of least-squares fitting of a parabola to the sample covariance function at small lags was first proposed in [9], in a discrete-time setting. However, explicit form of the estimator, such as the one given in (20), the bias analysis discussed in the previous paragraphs and summarized in (23) and (25), and the variance analysis, discussed in the next section, are not addressed in [9]. In the context of spectral moment estimation, closely related to our maximum Doppler estimation problem, utilization of the quadratic form of a correlation function at a *single* small lag, different from the MMSE formulation in (19), is discussed in [10] (see also [11] and [12]). Moreover, the bias/variance analysis of [10] is different from this paper and does not apply to the basic correlation function of interest in wireless communications, i.e.,  $J_0(\omega_d \tau)$ , which is not absolutely integrable. This important issue will be discussed later.

## B.2. Integration method

For an arbitrary real process  $y(t)$ , we know that  $r_y(\tau) = -r_y''(\tau)$  [7], where dot and prime denote differentiation with respect to the time  $t$  and the delay  $\tau$ , respectively. According to (15) and (16)

$$E[\dot{\xi}^2(t)] = \omega_d^2/4, \quad (26)$$

$$E[\dot{\eta}^2(t)] = \omega_d^2. \quad (27)$$

Now based on these two identities, one can consider the following estimator for  $\omega_d^2$

$$\widehat{\omega_{d,6}^2} = d \frac{1}{T} \int_0^T \dot{y}^2(t) dt, \quad (28)$$

where  $d = 4, 1$  for  $y(t) = \xi(t), \eta(t)$ , respectively. Note that unlike  $\widehat{\omega_{d,5}^2}$  in (20),  $\widehat{\omega_{d,6}^2}$  is an unbiased estimator for  $\omega_d^2$ . However,  $\widehat{\omega_{d,6}^2} = \sqrt{\omega_{d,6}^2}$  is clearly a biased estimator for  $\omega_d$ . To make a fair comparison between  $\widehat{\omega_{d,5}}$  in (21) and  $\widehat{\omega_{d,6}}$ , we use the same first-order Taylor expansion approximation, which yields

$$E[\widehat{\omega_{d,6}}] \approx \omega_d. \quad (29)$$

Eq. (28) was first proposed and substantially analyzed in [6], to estimate the spectral moment of a real Gaussian process. However, the envelope-squared non-Gaussian process is not considered in [6]. Furthermore, some of the conclusions made in [6] do not apply to the non-absolutely integrable correlation  $J_0(\omega_d \tau)$ . In addition, application of (28) to the envelope was first proposed in [13], without any statistical analysis. On the other hand, the estimators proposed in [14] and [15] can be considered as the discrete-time equivalent of (28), where integration is replaced by summation and  $\dot{y}(t)$  is approximated by the first-order difference  $[y((\ell+1)T_s) - y(\ell T_s)]/T_s$ , with  $\ell = 0, 1, \dots$ , and  $T_s$  as the sampling period.

## IV. ANALYTIC PERFORMANCE ANALYSIS

In this section we provide closed-form expressions for the variance of the inphase-based estimators discussed in the previous section. This has been possible due to the Gaussianity of  $\xi(t)$ . For the non-Gaussian envelope-squared process  $\eta(t)$ , it is very difficult, if not impossible, to derive closed-form results, and Monte Carlo simulation is the only resort. Throughout this section we consider an arbitrary PDF for the AOA in (3), which makes the results of this section applicable to any possible  $r_h(\tau)$ , and consequently,  $r_\xi(\tau)$ .

In what follows, we derive closed-form expressions for the variance of  $\xi(t)$ -based estimators  $\widehat{\omega_{d,1}}$ ,  $\widehat{\omega_{d,2}}$ ,  $\widehat{\omega_{d,5}}$ , and  $\widehat{\omega_{d,6}}$ . Then we show that as the observation time  $T$  increases, the variances of all these estimators converge to zero at the same rate of  $\ln(T)/T$ , where

$\ln(\cdot)$  is the natural logarithm. This novel result shows the asymptotic equivalence of these four estimators for any correlation function.

### A. Crossing-Based Methods

For a zero-mean, unit-variance, and real Gaussian  $\zeta(t)$ , the following result is given in [6] for the variance of  $(2\pi/T)N_\zeta(0, T)$ , the normalized number of zero upcrossings of  $\zeta(t)$  over  $(0, T]$

$$\text{Var}\left[\frac{2\pi}{T}N_\zeta(0, T)\right] = \frac{2\pi\gamma}{T} + \frac{2}{T} \int_0^T \left(1 - \frac{\tau}{T}\right) \times \left[ \frac{\sigma_\xi^2(\tau)}{\sqrt{1-r_\xi^2(\tau)}} \left\{ \sqrt{1-\rho_\xi^2(\tau)} + \rho_\xi(\tau) \cos^{-1}(-\rho_\xi(\tau)) \right\} - \gamma^2 \right] d\tau, \quad (30)$$

where  $r_\xi(\tau) = E[\zeta(t)\zeta(t+\tau)]$  and  $\gamma^2 = -r_\xi''(0)$ ,

$$\sigma_\xi^2(\tau) = \gamma^2 - r_\xi'^2(\tau)/[1-r_\xi^2(\tau)], \quad (31)$$

$$\sigma_\xi^2(\tau)\rho_\xi(\tau) = -r_\xi''^2(\tau) - r_\xi(\tau)r_\xi'^2(\tau)/[1-r_\xi^2(\tau)].$$

With  $\zeta(t) = \sqrt{2}\xi(t)$ , variance of  $\widehat{\omega_{d,1}}$  in (11) can be easily expressed in terms of (30). To calculate the variance of  $\widehat{\omega_{d,2}}$  in (12) using (30), we note that each maximum of  $\xi(t)$  corresponds to a zero downcrossing of the derivative  $\dot{\xi}(t)$ . Since the number of zero upcrossings and downcrossings are the same, we conclude that  $M_\xi(T) = N_\xi(0, T)$ . This, along with  $\zeta(t) = (2/\omega_d)\dot{\xi}(t)$  and  $r_\xi(\tau) = -r_\xi''(\tau)$ , gives the variance of  $\widehat{\omega_{d,2}}$  in closed form.

By extending the asymptotic analysis of [6] to our estimators, and using the asymptotic form of  $r_\xi(\tau)$ , given in [16], we have proved  $\text{Var}[\widehat{\omega_{d,1}}], \text{Var}[\widehat{\omega_{d,2}}] = O(T^{-1} \ln T)$ , as  $T \rightarrow \infty$ . (32)

This interesting new result, applicable to *any* correlation function, shows that for large observation intervals, the variance of both estimators converges to zero at the same rate.

### B. Covariance-Based Methods

#### B.1. Covariance matching method

Based on the forth-order moment of zero-mean and jointly Gaussian variables [7], and using the definition of the covariance estimator given in (22), it can be shown that

$$E[\widehat{c}_\xi(\tau_1)\widehat{c}_\xi(\tau_2)] = c_\xi(\tau_1)c_\xi(\tau_2) + \frac{1}{T} \int_{-T}^T \left(1 - \frac{|\tau|}{T}\right) \times [c_\xi(\tau)c_\xi(\tau+\tau_2-\tau_1) + c_\xi(\tau+\tau_2)c_\xi(\tau-\tau_1)] d\tau. \quad (33)$$

For  $\tau_1 = \tau_2$ , (33) simplifies to the result given in [17]. Using (23), it is straightforward to calculate the variance of  $\widehat{\omega_{d,5}^2}$ , defined in (20)

$$\text{Var}[\widehat{\omega_{d,5}^2}] = \left(\frac{5}{bT_0^5}\right)^2 \int_0^{T_0} \int_0^{T_0} \tau_1^2 \tau_2^2 \{E[\widehat{c}_\xi(\tau_1)\widehat{c}_\xi(\tau_2)] - c_\xi(\tau_1)c_\xi(\tau_2)\} d\tau_1 d\tau_2. \quad (34)$$

As before, we consider the first-order Taylor expansion [6] for  $\sqrt{\widehat{\omega_{d,5}^2}}$  around  $E[\widehat{\omega_{d,5}^2}] \neq \omega_d^2$ , which implies that

$$\text{Var}[\widehat{\omega_{d,5}}] \approx \text{Var}[\widehat{\omega_{d,5}^2}]/(4E[\widehat{\omega_{d,5}^2}]), \quad (35)$$

with the numerator and denominator given in (34) and (23), respectively.

If  $T_0$  is small enough, we can assume  $\widehat{\omega_{d,5}}$  is approximately unbiased, as shown in (25), and therefore  $\text{Var}[\widehat{\omega_{d,5}}]$  in (35) is enough to assess the performance. However, if the bias is not negligible, we need to look at the estimation error  $E[(\widehat{\omega_{d,5}} - \omega_d)^2] = \text{Var}[\widehat{\omega_{d,5}}] + (E[\widehat{\omega_{d,5}}] - \omega_d)^2$ . With  $T = 1$  sec. and uniform PDF for the AOA, i.e.,  $c_\xi(\tau)$  given by (15), the estimation

error of  $\hat{\omega}_{D,5}/(2\pi)$  is plotted in Fig. 1 versus  $T_0$ . COV in the legend box is the abbreviation for covariance and the subscript T stands for theoretical. Note that for each  $f_D$ , there is a single  $T_{0,opt}$  which yields the smallest estimation error. For  $T_0 < T_{0,opt}$ , the estimation error could be very large, specially for small  $f_D$  s. On the other hand, for each  $f_D$ , there is a neighborhood around  $T_{0,opt}$ , over which the estimation error remains almost constant. As  $f_D$  increases, this neighborhood becomes smaller.

At this moment, it seems difficult to study the asymptotic performance of  $\hat{\omega}_{D,5}$ , due to the complicated form of the estimator's bias, variance, and the parameter  $T_0$  involved. However, the indirect argument of [16], which takes advantage of the asymptotic properties of moment-based estimators, without deriving the variance expressions explicitly, might be applicable, which yields  $Var[\hat{\omega}_{D,5}] \approx O(T^{-1} \ln T)$ , as  $T \rightarrow \infty$ .

### B.2. Integration method

Based on [6], the variance of  $\hat{\omega}_{D,6}^2$  in (28) can be written as

$$Var[\hat{\omega}_{D,6}^2] = \frac{64}{T} \int_0^T \left(1 - \frac{\tau}{T}\right) r_{\xi}''^2(\tau) d\tau. \quad (36)$$

Again we consider the first-order Taylor expansion [6] for  $\sqrt{\hat{\omega}_{D,6}^2}$  around  $E[\hat{\omega}_{D,6}^2] = \omega_D^2$ , i.e.,  $Var[\hat{\omega}_{D,6}] \approx Var[\hat{\omega}_{D,6}^2]/(4E[\hat{\omega}_{D,6}^2])$ . Therefore

$$Var[\hat{\omega}_{D,6}] \approx \frac{16}{\omega_D^2 T} \int_0^T \left(1 - \frac{\tau}{T}\right) r_{\xi}''^2(\tau) d\tau. \quad (37)$$

Using the asymptotic form of  $r_{\xi}(\tau)$ , given in [16], it is easy to show that (37) yields

$$Var[\hat{\omega}_{D,6}] \approx O(T^{-1} \ln T), \text{ as } T \rightarrow \infty. \quad (38)$$

This interesting result, applicable to any correlation function, agrees with the result of [16], which was derived via a different approach and in a discrete-time setting.

## V. SIMULATION RESULTS AND PERFORMANCE COMPARISON

In this section we consider four inphase-based and four envelope-based estimators and compare their performance in terms of the estimation error. For the estimation error of the inphase-based methods, we have used the closed-form expressions presented in this paper (also verified by simulation but not shown in the figures), whereas the estimation error of the envelope-based techniques are obtained via simulation. Using the spectral method [18], 100 independent realizations of zero-mean (no LOS) complex Gaussian processes are generated, with  $N=10000$  complex samples per realization, which is equivalent to  $T=1$  sec. The simulated autocorrelation is given in (6). The spectral method is also used for generating the complex Gaussian bandlimited noise, with a flat power spectrum over the fixed receiver bandwidth of 101 Hz.

Note that in covariance matching, using either the inphase component or the envelope, we need to specify  $T_0$ . Since  $T_{0,opt}$  varies over a large range, as  $f_D$  changes, we have chosen  $T_0=0.005$  and  $0.06$  sec. from Fig. 1, for  $31 \leq f_D \leq 81$  and  $1 \leq f_D < 31$  Hz, respectively. This means that we are assuming a rough prior knowledge on the speed is available, when using the covariance matching method. Also note that choosing the appropriate  $T_0$  for the envelope-based covariance matching, from the inphase-based curves of Fig. 1, is convenient but not optimum. Clearly, there is no need to predetermine any parameter for the other six methods.

Fig. 2 - Fig. 4 show the estimation error of eight estimators  $\hat{f}_D = \hat{\omega}_D/(2\pi)$  versus  $f_D = \omega_D/(2\pi)$ . The abbreviations LCR, ROM, INT, COV, and ZCR in the legend boxes refer to the level crossing

rate, rate of maxima, integration, covariance, and zero crossing rate, respectively. In addition, the subscripts S and T stand for simulated and theoretical, respectively.

Based on Fig. 2, where we have isotropic scattering without noise, InphaseROM and EnvelopeROM demonstrate the best performance, whereas InphaseCOV and EnvelopeCOV are the worst. When including the effect of nonisotropic scattering without noise, depicted in Fig. 3, InphaseROM is the best and Envelope{LCR,INT,COV} are the worst for  $f_D \geq 10$  Hz, whereas InphaseCOV shows large errors when  $f_D < 10$  Hz. With isotropic scattering and a finite SNR of 10 dB, Fig. 4 shows the impact of noise. For large Dopplers, all the techniques do reasonably well in the presence of noise. One could also say that for medium and large Dopplers,  $f_D \geq 20$  Hz, InphaseZCR is the best choice. On the other hand, when  $f_D$  is small, InphaseCOV and EnvelopeCOV perform much better than the other techniques. This is due to the proper choice of the parameter  $T_0$  for small speeds.

## VI. CONCLUSION

In this paper we have studied a variety of crossing-based and covariance-based speed estimation techniques, in a unified framework. Such a framework has helped us to assess the performance of all the estimators, analytically, under the same umbrella, when the inphase component is used. As a byproduct of this approach, we have demonstrated, mathematically, that for large observation intervals, the performance of all these estimators is the same. Closed-form expressions for the bias and variance of the inphase-based estimators are also derived and verified via simulation. We have observed that when noise is negligible, rate of maxima of the inphase component and also the envelope provide the best performance. Rate of maxima of the inphase component also remains to be best in the presence of nonisotropic scattering. When noise is not negligible and speed is high, most of the methods show a good performance. In particular, for medium and high speeds, the zero crossing rate of the inphase component is the best choice. However, for small speeds, only the covariance matching technique provides an accurate estimate, when noise is present.

## REFERENCES

- [1] C. Tepedelenlioglu, A. Abdi, G. B. Giannakis, and M. Kaveh, "Estimation of Doppler spread and signal strength in mobile communications with applications to handoff and adaptive transmission," *Wirel. Commun. Mob. Comput.*, vol. 1, pp. 221-242, 2001.
- [2] A. Abdi and M. Kaveh, "Parametric modeling and estimation of the spatial characteristics of a source with local scattering," in *Proc. IEEE Int. Conf. Acoust., Speech, Signal Processing*, Orlando, FL, 2002, pp. 2821-2824.
- [3] A. Abdi, J. A. Barger, and M. Kaveh, "A parametric model for the distribution of the angle of arrival and the associated correlation function and power spectrum at the mobile station," *IEEE Trans. Vehic. Technol.*, vol. 51, pp. 425-434, 2002.
- [4] J. D. Parsons, *The Mobile Radio Propagation Channel*, 2nd ed., Chichester, England: Wiley, 2000.
- [5] G. L. Stuber, *Principles of Mobile Communication*, 2nd ed., Boston, MA: Kluwer, 2001.
- [6] G. Lindgren, "Spectral moment estimation by means of level crossings," *Biometrika*, vol. 61, pp. 401-418, 1974.
- [7] A. Papoulis, *Probability, Random Variables, and Stochastic Processes*, 3rd ed., Singapore: McGraw-Hill, 1991.
- [8] A. Abdi and S. Nader-Esfahani, "Expected number of maxima in the envelope of a spherically invariant random process," *IEEE Trans. Inform. Theory*, vol. 49, pp. 1369-1375, 2003.
- [9] C. Tepedelenlioglu and G. B. Giannakis, "On velocity estimation and correlation properties of narrow-band mobile communication channels,"

- IEEE Trans. Vehic. Technol.*, vol. 50, pp. 1039-1052, 2001.
- [10] K. S. Miller and M. M. Rochwarger, "A covariance approach to spectral moment estimation," *IEEE Trans. Inform. Theory*, vol. 18, pp. 588-596, 1972.
- [11] K. S. Miller and M. M. Rochwarger, "Some remarks on spectral moment estimation," *IEEE Trans. Commun.*, vol. 20, pp. 260-262, 1972.
- [12] K. S. Miller, *Complex Stochastic Processes: An Introduction to Theory and Application*. Reading, MA: Addison-Wesley, 1974.
- [13] P. P. A. Bello, "Some techniques for the instantaneous real-time measurement of multipath and Doppler spread," *IEEE Trans. Commun. Technol.*, vol. 13, pp. 285-292, 1965.
- [14] J. M. Holtzman and A. Sampath, "Adaptive averaging methodology for handoffs in cellular systems," *IEEE Trans. Vehic. Technol.*, vol. 44, pp. 59-66, 1995.
- [15] J. M. Perl and D. Kagan, "Real-time HF channel parameter estimation," *IEEE Trans. Commun.*, vol. 34, pp. 54-58, 1986.
- [16] C. Tepedelenlioglu, "Performance analysis of velocity (Doppler) estimators in mobile communications," in *Proc. IEEE Int. Conf. Acoust., Speech, Signal Processing*, Orlando, FL, 2002, pp. 2201-2204.
- [17] J. S. Bendat and A. G. Piersol, *Measurement and Analysis of Random Data*. New York: Wiley, 1966.
- [18] K. Acolatse and A. Abdi, "Efficient simulation of space-time correlated MIMO mobile fading channels," to be published in *Proc. IEEE Vehic. Technol. Conf.*, Orlando, FL, 2003.

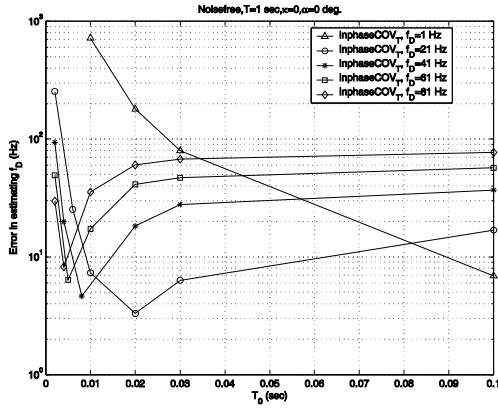


Fig. 1. Estimation error (in Hz) of the covariance matching method using the inphase component, versus the parameter  $T_0$ , assuming isotropic scattering.

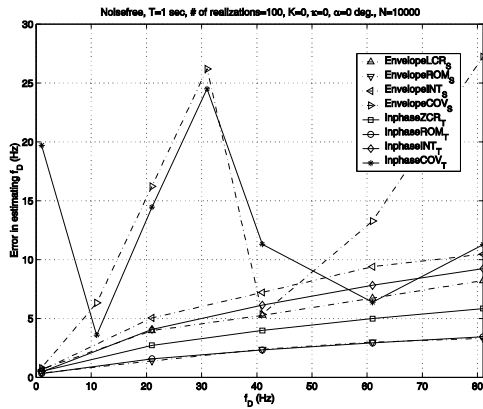


Fig. 2. Estimation error of eight estimators versus the maximum Doppler frequency (no noise and isotropic scattering).

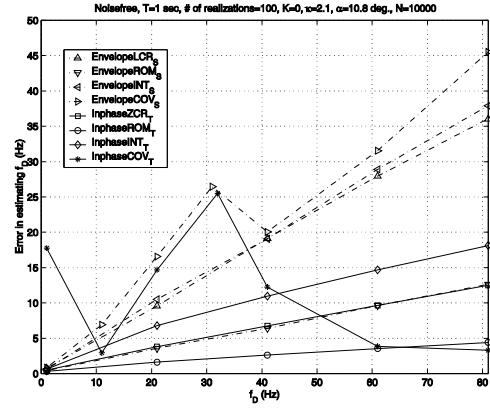


Fig. 3. Estimation error of eight estimators versus the maximum Doppler frequency (no noise and nonisotropic scattering).

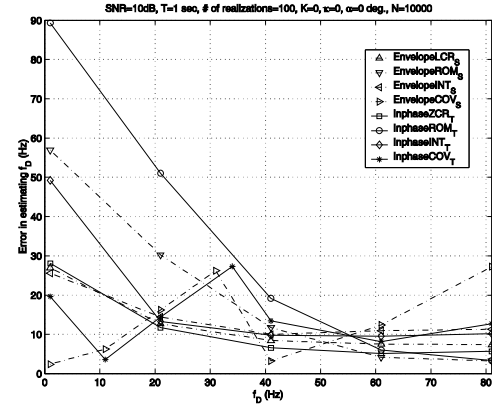


Fig. 4. Estimation error of eight estimators versus the maximum Doppler frequency (SNR = 10 dB and isotropic scattering).